Mineralogical Magazine, August 2018, Vol. 82(4), pp. 821–836

Folvikite, $Sb^{5+}Mn^{3+}(Mg,Mn^{2+})_{10}O_8(BO_3)_4$, a new oxyborate mineral from the Kitteln mine, Nordmark ore district, Värmland, Sweden: description and crystal structure

Mark A. Cooper[1], Gunnar Raade[2], Neil A. Ball[1], Yassir A. Abdu[1], Frank C. Hawthorne[1,*] and Ralph Rowe[3]

[1] Department of Geological Sciences, University of Manitoba, Winnipeg, Manitoba R3 T 2N2, Canada
[2] Natural History Museum, University of Oslo, PO Box 1172 Blindern, NO–0318 Oslo, Norway
[3] Canadian Museum of Nature, PO Box 3443 Stn D, Ottawa, Ontario K1P 6P4, Canada

[*Received 28 April 2017; Accepted 4 July 2017; Associate Editor: Andrew Christy*]

ABSTRACT

Folvikite, $Sb^{5+}Mn^{3+}(Mg,Mn^{2+})_{10}O_8(BO_3)_4$, is a new oxyborate mineral from the Kitteln mine, Värmland, Sweden, where it occurs as a primary skarn mineral embedded in calcite. It forms striated prismatic crystals up to 0.3 mm, and is black to dark reddish-brown with submetallic lustre and a reddish-brown streak. It is brittle, has a Mohs hardness of 6, and the calculated density is 4.14 g/cm^3. Folvikite is biaxial with indeterminate optic sign due to pervasive twinning. The optic axial angle is 68.9(4)°. Refractive indices were not measured; the calculated mean refractive index is 1.85. Strong pleochroism was observed in plane-polarized light: AB = brown (intermediate), OB = dark brown (maximum) and ON = honey brown (minimum). Folvikite is monoclinic, space group $P2$, $a = 5.3767(10)$, $b = 6.2108(10)$, $c = 10.9389(18)$ Å, $\beta = 94.399(9)°$, $V = 364.22(16)$ Å^3 and $Z = 1$. Chemical analysis by electron microprobe gave Sb_2O_5 18.15, MgO 24.11, MnO 29.73, Mn_2O_3 11.62, Al_2O_3 0.27, Fe_2O_3 0.45, B_2O_3 15.27, sum 99.60 wt.%. The B_2O_3 content was assigned as B = 4 apfu and the Mn_2O_3 / (MnO + Mn_2O_3) ratio was determined from the crystal structure. The empirical formula was normalized on the basis of 20 anions pfu: $(Sb^{5+}_{1.02}Mn^{3+}_{1.34}Al_{0.05}Fe^{3+}_{0.05}Mg_{5.46}Mn^{2+}_{3.82}\square_{0.26})_{\Sigma 12}O_8(BO_3)_4$. A simplified formula may be written as $Sb^{5+}Mn^{3+}(Mg,Mn^{2+})_{10}O_8(BO_3)_4$ with $Z = 1$. The crystal structure was solved by direct methods and refined to an R_1 index of 4.1%. Folvikite is a member of the (3 Å) zigzag wallpaper-borate structures in which chains of edge-sharing octahedra extend along the **c** axis and are cross-linked by BO_3 groups. There are five *X* sites partly occupied by Mn^{2+} > Mg, one octahedrally coordinated *M*-site occupied by Sb^{5+} > Mg, two *M* sites occupied by Mg ≥ Mn > Sb^{5+}, two *M* sites occupied by Mn^{3+} > Mn^{2+}, two *M* sites occupied by Mg > Mn^{2+}, and one *M*-site occupied by Mg > □; plus two [3]-coordinated *B* sites occupied by B. As with the other zigzag borates, the polyhedra are arranged in F-walls, C-walls and S-columns.

Keywords: folvikite, new mineral, chemical analysis, crystal structure, infrared spectrum, Kitteln mine, Värmland, Sweden.

Introduction

Folvikite is a new Sb-bearing oxyborate mineral of the 'pinakiolite group' of Strunz and Nickel (2001). It was found at the Kitteln mine of the Nordmark ore field, north of Filipstad, Värmland, Sweden (59°49'59"N, 14°05'59"E). The Kitteln mine is also the type locality for the Sb-bearing oxyborate blatterite (Raade *et al.*, 1988; Cooper and Hawthorne, 1998).

The mineral is named after Harald O. Folvik (born 1941). Mr. Folvik is a prominent Norwegian amateur mineralogist who has a particular interest in Långban-type deposits and is a member of The Långban Society. The mineral described here was noticed initially by him, and he collected the specimens that

*E-mail: frank_hawthorne@umanitoba.ca
https://doi.org/10.1180/minmag.2017.081.059

were used in this work. Both the mineral and the name have been approved by the Commission on New Minerals, Nomenclature and Classification of the International Mineralogical Association (IMA2016-026). The polished mount used for electron probe microanalysis is kept at the Natural History Museum, University of Oslo, Norway (catalogue number 43574). The crystal used for the structural study, powdered material used for IR spectroscopy and subsequent powder X-ray diffraction and the rock piece that yielded this material were deposited at the Canadian Museum of Nature, Ottawa (catalogue number CMNMC 87087).

Occurrence

The mines of the Nordmark ore field (Magnusson, 1929) were essentially worked for iron ore. Manganese ores were produced from two small mines: Östra Mossgruvan and Kitteln. The manganese ore at Östra Mossgruvan, originally mined for iron, was discovered in 1876 and consisted mainly of hausmannite with grains of manganosite (Sjögren, 1876, 1878). Production of manganese ore at the Kitteln mine, also at first mined for iron, began in 1887, and the ore was similar to that from Östra Mossgruvan (Sjögren, 1887).

The folvikite-bearing rock material in the Kitteln mine, as well as the blatterite-bearing material, was evidently dumped there from elsewhere. In the description of blatterite, Brattforsgruvan was tentatively suggested as the most probable source, based on the fact that katoptrite occurs with blatterite at Kitteln, and Brattforsgruvan is the type locality of that mineral. However, manganese ore has not, as far as we know, been reported from Brattforsgruvan, and Östra Mossgruvan is more likely to be the source. The distance between Kitteln and Östra Mossgruvan is only ~130–140 m. It is also conceivable that the backfill originates from the Kitteln mine itself. Considering this uncertainty, the Kitteln mine, where the material was collected, should be regarded as the type locality of both blatterite and folvikite.

Associated minerals

Folvikite occurs embedded in calcite. Other minerals identified in the assemblage are hausmannite, tegengrenite and a Mg-dominant analogue of sonolite or jerrygibbsite, $(Mg,Mn)_9(SiO_4)_4(OH)_2$; the latter species may occur as inclusions in folvikite. Blatterite and folvikite do not occur together, blatterite being confined to manganosite-bearing ore.

Physical properties

Folvikite forms strongly lustrous, elongate prismatic crystals up to 0.3 mm long. They are commonly striated along their length due to twinning by 180° rotation about **c***; an aggregate, 0.1 mm wide, of five parallel individuals, was reported by Raade and Folvik (2013). Crystals are elongated along [010] with indeterminate interpenetrating {*h*0*l*} forms (Fig. 1). Folvikite is black to dark reddish-brown with a reddish-brown streak. It has a submetallic lustre and the diaphaneity is generally opaque except at thin edges where the colour is dark red-brown. Cleavage and parting were not observed, folvikite is brittle and has conchoidal fracture. Mohs hardness is 6, and folvikite does not luminesce in ultraviolet light. The calculated density is 4.14 g/cm^3 (from the empirical formula). Folvikite is biaxial with indeterminate optic sign due to pervasive twinning. The optical axial angle was measured with a spindle stage using the program *Excalibr2* (Bartelmehs *et al*., 1992) and is 68.9(4)°. Refractive indices were not measured; the calculated mean refractive index is 1.85. The long axis of the crystal is parallel to the optic normal and hence $Y = b$. Strong pleochroism was observed in plane-polarized light: AB = brown (intermediate), OB = dark brown (maximum) and ON = honey brown (minimum).

Chemical composition

Crystals were analysed with a Cameca SX100 electron microprobe (EMPA) operated in wavelength-dispersive mode at 15 kV and 15 nA and using a beam diameter of 1 μm. Concentrations of Ca and Ti were below the detection limits of EMPA.

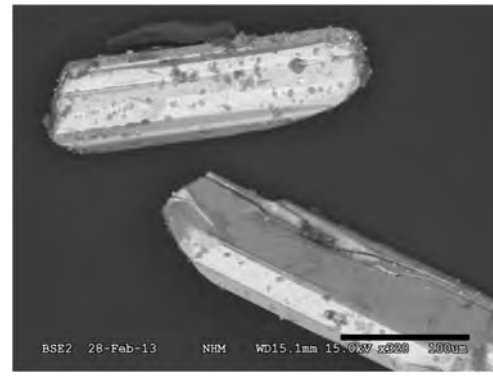

FIG. 1. Back-scattered electron image of crystals of folvikite; note the interpenetrating forms.

The following standards were used: Sb_2S_3 (Sb), MgO (Mg), pyrophanite (Mn), Al_2O_3 (Al) and Fe metal (Fe). Boron was analysed by electron counting during crystal-structure refinement (Hawthorne and Grice, 1990), and its presence in the structure was also confirmed by infrared spectroscopy (see below). Lithium is below detection using LA-ICP-MS (laser ablation inductively coupled plasma mass spectrometry). Table 1 gives the chemical composition (mean of seventeen points from three grains). The empirical formula unit, calculated to give a cation sum (excluding B) of 11.74 apfu with B = 4 apfu (atoms per formula unit) is: $(Sb^{5+}_{1.02}Mn^{3+}_{1.34}Al_{0.05}Fe^{3+}_{0.05}Mg_{5.46}Mn^{2+}_{3.82}\square_{0.26})_{\Sigma 12}O_8(BO_3)_4$; the simplified formula is $Sb^{5+}Mn^{3+}(Mg,Mn^{2+})_{10}O_8(BO_3)_4$ ($Z = 1$) (see later discussion for justification of this procedure).

Infrared spectroscopy

The Fourier-transform infrared (FTIR) spectrum was collected using a Bruker Hyperion 2000 IR microscope equipped with a liquid-nitrogen-cooled mercury-cadmium-telluride detector. The spectrum in the range 4000–650 cm^{-1} was obtained by averaging 100 scans with a resolution of 4 cm^{-1}. The infrared spectrum of folvikite is shown in Fig. 2. The spectrum shows no absorption bands in the OH-stretching region (4000–3000 cm^{-1}), which is in accord with the absence of OH groups and H_2O in the structure. Absorption bands in the region 1500–900 cm^{-1} (with strong bands at 1335, 1275 and 1240 cm^{-1}, and medium to low intensity bands at 1124, 948, 934 and 906 cm^{-1}) may be assigned to B–O stretching vibrations of the borate group. Bands at 723 and 666 cm^{-1} are due to bending modes of the borate group.

TABLE 1. Chemical composition (wt.%) of folvikite.

Constituent	Wt.%	Range
Sb_2O_5	18.15(32)	17.31–18.55
MgO	24.11(66)	22.79–25.06
MnO^{tot}	40.17(89)	39.04–41.64
MnO	29.73	
Mn_2O_3*	11.62	
Al_2O_3	0.27(2)	0.24–0.31
Fe_2O_3	0.45(6)	0.36–0.59
B_2O_3**	15.27	
Total	99.60	

Below detection: Ca and Ti (EMPA); Li (LA-ICP-MS);
*calculated to give a cation sum (excluding B^{3+}) of 11.74 apfu;
**calculated to give $B^{3+} = 4$ apfu.

Powder X-ray diffraction

The powder-diffraction pattern for folvikite was recorded at the Canadian Museum of Nature using a Bruker D8 Discover micro-powder diffractometer with a Hi-Star multi-wire 2D detector at 12 cm, calibrated following Rowe (2009) and using a pseudo-Gandolfi approach on a powdered sample of folvikite that was crushed using a diamond micro-anvil. The unit-cell dimensions were refined using the program *UNITCELL* of Holland and Redfern (1995). The powder pattern is given in Table 2, together with the refined cell-dimensions which are in close accord with the values derived by single-crystal X-ray diffraction.

Crystal structure: data collection, structure solution and refinement

A single (twinned) crystal (5 μm x 6 μm x 40 μm) was attached to a tapered glass fibre and mounted on a Bruker D8 three-circle diffractometer equipped with a rotating anode generator (Mo$K\alpha$ X-radiation), multilayer optics and an APEX-II detector. In excess of a Ewald sphere of data was collected to 60°2θ using 26 s per 0.2° frame with a crystal-detector distance of 8 cm. A preliminary evaluation of the diffraction pattern at a crystal-detector distance of 5 cm showed that the crystal contained a significant non-merohedral twin component [twin law: 180° rotation about **c***], and the detector was moved back to 8 cm to further enhance resolution of the partly overlapping twin component. Twin integration gave 30,684 total reflections, with 11,869 [component 1], 11,935 [component 2] and 6880 [both components] constituent reflections. The reflections were averaged and merged [$R_{int} = 5.8\%$] to give 1166 reflections (single reflections from the primary domain, plus composites involving both domains) for structure (twin) refinement. The unit-cell dimensions were obtained by least-squares refinement of 7131 reflections with $I > 10\sigma I$.

An oriented 'precession' slice ($h0l$) was constructed from the raw data frames and is shown in Fig. 3; the diffraction spots from the primary domain (green $h0l$ labelling) are related to the diffraction spots from the twin domain (red $h0l$ labelling) by a 180° rotation about **c***. Note the different inter-spot spacing along **c*** for different

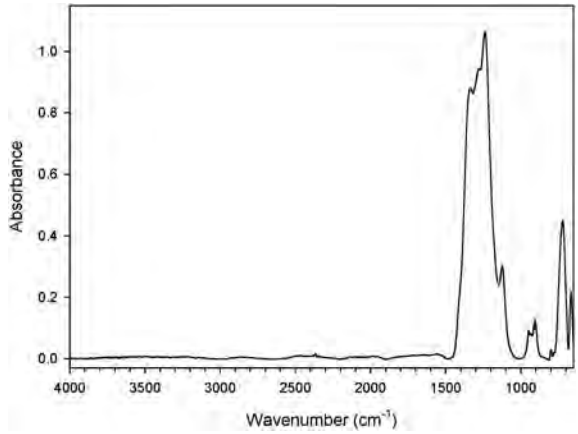

FIG. 2. The FTIR spectrum of folvikite.

TABLE 2. X–ray powder diffraction pattern** of folvikite.

I_{obs} %	I_{SXL} %	d_{SXL} Å	d_{obs} Å	d_{calc} Å	*h k l*
100	100	5.453	**5.450**	5.450	0 0 2
	34	5.361			1 0 0
46	46	4.964	**4.973**	4.972	$\bar{1}$ 0 1
12	14	3.684	3.688	3.687	1 0 2
32	34	3.106	3.112	3.110	0 2 0
10	11	2.907	2.907 *		1 0 3
82	95	2.727	**2.725**	2.725	0 0 4
	24	2.699			0 2 2
91	56	2.586	**2.591**	2.590	1 2 1
31	43	2.482	2.486	2.486	$\bar{2}$ 0 2
15	12	2.448	2.450	2.451	$\bar{1}$ 2 2
24	15	2.375	2.375	2.377	1 2 2
9	10	2.336	2.338	2.339	2 0 2
8	7	2.202	2.201	2.204	$\bar{1}$ 2 3
13	22	2.181	2.183	2.180	0 0 5
12	7	2.122	2.124	2.124	1 2 3
43	35	2.029	**2.033**	2.033	2 2 0
	13	2.016			$\bar{2}$ 2 1
5	16	1.989	1.991	1.991	$\bar{2}$ 0 4
3	3	1.939	1.940	1.942	$\bar{2}$ 2 2
15	10	1.878	1.880	1.879	1 2 4
11	9	1.675	1.672 *		$\bar{2}$ 2 4
15	15	1.663	1.662	1.663	1 2 5
15	15	1.584	1.585	1.586	2 2 4
	18	1.561			$\bar{2}$ 0 6
37	42	1.553	**1.552** *		0 4 0
14	17	1.533	1.532	1.533	$\bar{1}$ 2 6

$a = 5.388(2)$, $b = 6.220(2)$, $c = 10.933(3)$ Å, $\beta = 94.40(3)°$ and $V = 365.27(15)$ Å^3
*Excluded in least–squares refinement; **the subscript SXL denotes single-crystal diffraction data.
The six strongest lines are given in bold.

values of H; complete overlap occurs for (00*l*) reflections, and nearly so for (*h*0*l*) reflections with H = 3 and –3. All diffraction maxima from the X-ray crystal can be indexed on the small monoclinic cell (5.38 × 6.21 × 10.94 Å) with the inclusion of the twin law. Structure (twin) refinement from 1166 reflections (including 607 composites) gave a final R_1 value of 4.1% (for 1070 observed reflections, $|F_o| > 4\sigma F$). The Flack parameter refined to –0.03 (16), indicating a correct absolute structural configuration. The twin volume fraction (i.e. twin contribution to composites) refined to 0.417(2), suggesting a very significant twin fraction (as is indicated on the precession slice in Fig. 3). Miscellaneous information concerning structure solution and refinement is listed in Table 3. Atom positions and displacement parameters are given in Table 4, selected interatomic distances in Table 5, site-scattering values and site assignments in Table 6 and a bond-valence calculation in Table 7. The crystallographic information files have been deposited with the Principal Editor of *Mineralogical Magazine* and are available as Supplementary material (see below).

Crystal structure: site assignment and formula normalization

The crystal structure of folvikite contains both positionally ordered *M*-cations (octahedral coordination), positionally disordered *X*-cations (coordination numbers [4], [5] and [6]), and ordered BO_3 groups. There are eight *M*-cation sites and five *X*-cation sites, and all give refined site-scattering values (Hawthorne *et al*., 1995) that suggest multiple occupants at each of these sites. There are primarily five constituents to assign over the thirteen (*M* + *X*) sites: Sb^{5+}, Mg^{2+}, Mn^{2+}, Mn^{3+} and □ (vacancy); we combined the minor Al^{3+} and Fe^{3+} contents from the chemical data with Mn^{3+} on the basis of their similar charge and radii (Shannon, 1976).

As the structure of folvikite contains the same architectural elements as in other zigzag borates (i.e. F- and C-walls; and S-columns; Cooper and Hawthorne, 1998), we use many of the same general crystal-chemical arguments to help assign cations in the folvikite structure. The *M* sites in folvikite have refined site-scattering values spanning the range 8.9–41.6 epfu (electrons per formula unit), and a vacancy (□) must be associated with at least one of these sites, as Mg (12 electrons) is the weakest X-ray scattering species present. With a known vacancy present for at least one *M*-site, and additionally at the positionally disordered *X* sites, the overall cation sum for folvikite is not fixed. An additional variable involves the partitioning of Mn as Mn^{2+} and Mn^{3+}. The most feasible approach to normalizing the chemical data therefore involves an anion-normalization scheme [i.e. $(BO_3)_4O_8 = 28^-$], with an assessment of both the vacancy content and the Mn^{2+}/Mn^{3+} ratio via crystal-chemical arguments from the structure refinement. The *M*(1) site has the largest refined site-scattering value (41.6 epfu) and the shortest mean bond length (<*M*(1)–O> = 2.019 Å) of all the *M* sites and must contain significant Sb^{5+} (Table 6). Note that there is no Sb^{3+} present in folvikite, as Sb^{3+} is a lone-pair stereoactive cation that has very different stereochemistry that we do not observe here (Mills *et al*., 2009). The *M*(2) site has the lowest refined site-scattering value (8.9 epfu) and a <*M*(2)–O> distance of 2.119 Å; without knowing the constituent size of a vacancy, or whether there is more than one type of cation present, the simplest assignment to be made for the *M*(2) site involves Mg + vacancy (Table 6). The next two smallest *M*-octahedra involve the *M*(4) and *M*(5) sites with <*M*(4)–O> = 2.065 Å and <*M*(5)–O> = 2.071 Å; the refined site-scattering values for these two sites (~23 epfu), in combination with the observed <*M*–O> distances, suggest dominant Mn^{3+}. In addition, by comparison with other zigzag borate structures, we expect these edge-sharing [= *M*(4) = *M*(5) =] strips of octahedra within the C-wall to be occupied by Jahn-Teller-distorted Mn^{3+} octahedra. Most of the pinakiolite-group minerals contain [4 + 2]-distorted Mn^{3+}-bearing octahedra with four short and two long bonds; however in folvikite, the Mn^{3+} octahedra show [2 + 2 + 2] distortion (i.e. two short, two intermediate and two long bonds) and are occupied by ~33% other cations. This situation is analogous to that of the *M*(4) octahedron in fredrikssonite (Burns *et al*., 1994) in which a similar [2 + 2 + 2] distortion occurs and the *M*(4) site is occupied primarily by Mn^{3+} with ~22% other cations. The cations Mg, Mn^{2+} and minor Sb^{5+} were assigned to the remaining *M* sites [*M*(3), *M*(6), *M*(7) and *M*(8)] in folvikite in accord with the relative site-scattering values and observed bond lengths. The positionally disordered *X* sites adjacent to the Jahn-Teller-distorted Mn^{3+} octahedral strips of the C-wall are considered to be occupied predominately by Mn^{2+}, with subordinate Mg. There are five *X* sites in total, and we propose maximum occupancy for this region of the structure (i.e. 2 apfu), whereby close *X*–*X*′ contacts preclude local mutual occupancy of many *X*–*X*′ pairs.

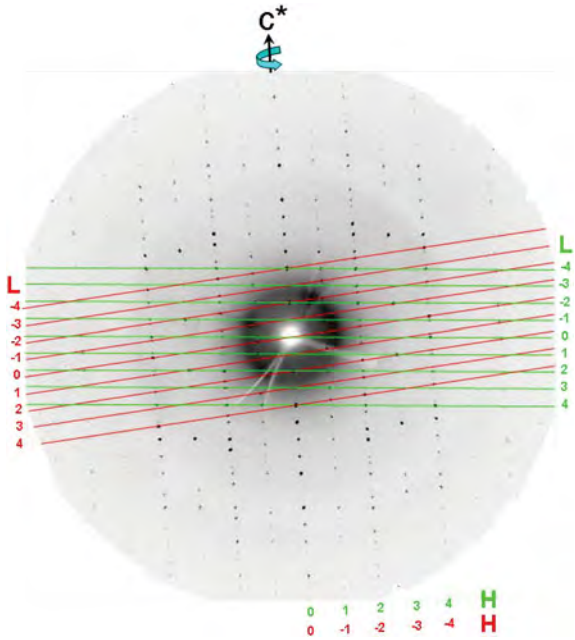

FIG. 3. The (*h*0*l*) precession layer for folvikite generated from the single-crystal X-ray diffraction data. Twin law = 180° rotation about **c***. Primary-domain indexing in green and twin-component indexing in red.

The total refined site-scattering at all ($M+X$) sites is 247.3 epfu [$Z=1$], in good agreement with the scattering value of 248.7 epfu calculated for the chemical formula derived from electron-microprobe analysis. The chemical data were normalized to 20 O^{2-} anions, with 4 B apfu, i.e. $[O_8(BO_3)_4] = 28^-$, with a $Mn^{3+}/(Mn^{3+}+Mn^{2+})$ value adjusted to give an [$M+X$] cation sum of 11.74 apfu [i.e. 12.00–0.26 $^{M(2)}\square$]. The constituent radii for the *M*-site assignments are plotted against the observed <*M*–O> distances in Fig. 4, and a linear regression gives <*M*–O> = 0.834 (*r*) + 1.497 Å. A similar regression line constructed for the octahedrally coordinated sites in blatterite gave <*M*–O> = 0.8325 (*r*) + 1.5060 (Cooper and Hawthorne, 1998), and the congruency between the two relations supports the site assignments for these two homologous structures. Finally, the incident bond-valence sums at the *M* sites (Table 7) are in close accord with the aggregate formal charge of the constituent cations at these sites, with a mean deviation of 0.07. Moreover, the incident bond-valence sums at the *B* sites (Table 7) are in accord with their occupancy by B^{3+}.

TABLE 3. Miscellaneous information concerning data collection and structure refinement for folvikite.

a (Å)	5.3767(10)
b	6.2108(10)
c	10.9389(18)
β (°)	94.399(9)°
V (Å^3)	364.22(16)
Space group	*P*2
Z	4
D_{calc} (g/cm^3)	4.14
Crystal size (μm)	5 × 6 × 40
Radiation	Mo*K*α
No. of reflections	30,684
No. unique reflections	1166
R_{int} %	5.8
No. with ($Fo > 4\sigma F$)	1070
R_1 %	4.1
wR_2 %	8.0
Goof	1.103
Parameters/restraints	127/1

$R_1 = \Sigma(|Fo| - |Fc|) / \Sigma|Fc|$
$wR_2 = [\Sigma w(F_o^2 - F_c^2)^2 / \Sigma w(F_o^2)^2]^{1/2}$, $w = 1 / [\sigma^2(F_o^2) + (0.0122\,P)^2 + 3.90\,P]$ where $P = (\max(F_o^2,0) + 2F_c^2) / 3$

Crystal structure: description

As the structure of folvikite is related closely to the structure of pinakiolite, we describe its relation to its closest structural (and chemical)

TABLE 4. Atom positions and equivalent isotropic-displacement parameters (Å^2) for folvikite.

Site	*x*	*y*	*z*	U_{eq}	U^{11}	U^{22}	U^{33}	U^{23}	U^{13}	U^{12}
M(1)	½	0.9064(4)	0	0.0038(3)	0.0018(4)	0.0048(4)	0.0047(5)	0	0.0006(4)	0
M(2)	0	0.168(2)	0	0.014(4)	0.017(6)	0.002(4)	0.024(7)	0	−0.001(6)	0
M(3)	½	0.4093(13)	0	0.0128(7)	0.0118(10)	0.0111(10)	0.0155(12)	0	0.0011(10)	0
M(4)	0	0.4069(11)	½	0.0093(6)	0.0093(9)	0.0077(9)	0.0103(10)	0	−0.0025(7)	0
M(5)	½	0.4048(10)	½	0.0100(6)	0.0107(9)	0.0071(9)	0.0127(10)	0	0.0036(7)	0
M(6)	0	0.6521(12)	0	0.0101(15)	0.007(2)	0.017(2)	0.007(2)	0	0.003(2)	0
M(7)	0.7176(8)	0.6574(7)	0.2767(2)	0.0078(9)	0.0071(19)	0.0082(14)	0.0083(16)	0.001(3)	0.0018(17)	−0.003(3)
M(8)	0.7166(8)	0.1597(7)	0.2760(2)	0.0099(9)	0.0112(19)	0.0106(14)	0.0078(15)	0.000(3)	0.0011(17)	−0.003(3)
X(1)	½	0.911(3)	½	0.007(2)						
X(2)	0.401(2)	0.907(4)	0.4834(7)	0.008(3)						
X(3)	0.241(2)	0.904(4)	0.4524(7)	0.017(3)						
X(4)	0	0.912(3)	½	0.007(2)						
X(5)	0.098(3)	0.908(5)	0.4866(9)	0.008(4)						
B(1)	0.207(2)	0.409(5)	0.2295(8)	0.0080(14)						
B(2)	0.212(2)	0.910(6)	0.2387(9)	0.0130(17)						
O(1)	0.9946(11)	0.406(3)	0.2926(6)	0.0111(13)						
O(2)	0.4415(11)	0.412(3)	0.2905(5)	0.0103(13)						
O(3)	0.1826(13)	0.407(3)	0.1018(5)	0.0076(11)						
O(4)	0.9950(11)	0.908(3)	0.2966(6)	0.0111(12)						
O(5)	0.4487(11)	0.912(3)	0.2978(6)	0.0123(13)						
O(6)	0.1946(14)	0.904(3)	0.1069(5)	0.0097(12)						
O(7)	0.677(2)	0.1375(18)	0.0909(8)	0.009(2)						
O(8)	0.685(2)	0.663(2)	0.0885(8)	0.009(2)						
O(9)	0.7463(19)	0.6081(14)	0.4709(7)	0.0060(16)						
O(10)	0.7446(19)	0.1595(19)	0.4727(7)	0.0105(18)						

TABLE 5. Selected interatomic distances (Å) in folvikite.

M(1)–O(6) ×2	2.088(7)	*X*(1)–O(5) ×2	2.208(6)
M(1)–O(7) ×2	1.952(11)	*X*(1)–O(9) ×2	2.336(18)
M(1)–O(8) ×2	2.017(12)	*X*(1)–O(10) ×2	2.064(19)
<*M*(1)–O>	2.019	<*X*(1)–O>	2.203
M(2)–O(3) ×2	2.056(17)	*X*(2)–O(5)	2.067(10)
M(2)–O(6) ×2	2.228(18)	*X*(2)–O(5)	2.467(11)
M(2)–O(7) ×2	2.074(12)	*X*(2)–O(9)	2.09(2)
<*M*(2)–O>	2.119	*X*(2)–O(10)	1.83(2)
		X(2)–O(10)	2.43(2)
M(3)–O(3) ×2	2.108(7)	<*X*(2)–O>	2.18
M(3)–O(7) ×2	2.145(14)		
M(3)–O(8) ×2	2.062(14)	*X*(3)–O(4)	2.075(11)
<*M*(3)–O>	2.105	*X*(3)–O(5)	2.098(11)
		X(3)–O(9)	2.02(2)
M(4)–O(1) ×2	2.267(6)	*X*(3)–O(10)	1.78(3)
M(4)–O(9) ×2	1.860(10)	<*X*(3)–O>	1.99
M(4)–O(10) ×2	2.067(11)		
<*M*(4)–O>	2.065	*X*(4)–O(4) ×2	2.223(6)
		X(4)–O(9) ×2	2.336(17)
M(5)–O(2) ×2	2.290(6)	*X*(4)–O(10) ×2	2.068(18)
M(5)–O(9) ×2	1.875(10)	<*X*(4)–O>	2.209
M(5)–O(10) ×2	2.049(11)		
<*M*(5)–O>	2.071	*X*(5)–O(4)	2.110(11)
		X(5)–O(4)	2.461(12)
M(6)–O(3) ×2	2.088(13)	*X*(5)–O(9)	2.08(3)
M(6)–O(6) ×2	2.174(14)	*X*(5)–O(10)	1.81(3)
M(6)–O(8) ×2	2.016(12)	*X*(5)–O(10)	2.46(2)
<*M*(6)–O>	2.093	<*X*(5)–O>	2.18
M(7)–O(1)	2.156(16)	*B*(1)–O(1)	1.377(11)
M(7)–O(2)	2.142(15)	*B*(1)–O(2)	1.383(11)
M(7)–O(4)	2.153(16)	*B*(1)–O(3)	1.393(10)
M(7)–O(5)	2.167(17)	<*B*(1)–O>	1.384
M(7)–O(8)	2.053(9)		
M(7)–O(9)	2.140(7)	*B*(2)–O(4)	1.371(13)
<*M*(7)–O>	2.135	*B*(2)–O(5)	1.382(13)
		B(2)–O(6)	1.438(11)
M(8)–O(1)	2.136(16)	<*B*(2)–O>	1.397
M(8)–O(2)	2.168(16)		
M(8)–O(4)	2.166(16)		
M(8)–O(5)	2.134(16)		
M(8)–O(7)	2.025(9)		
M(8)–O(10)	2.145(7)		
<*M*(8)–O>	2.129		

relative: Sb-rich pinakiolite from Långban, Sweden (Hansen *et al.*, 1988; Norrestam and Hansen, 1990). Folvikite and Sb-rich pinakiolite share the same style of structural connectivity, but differ in terms of unit cell and space group: folvikite crystallizes in *P*2 and has a cell volume half that of Sb-rich pinakiolite which crystallizes in *C*2/*m*.

F-walls

In the crystal structure of folvikite, *M*(1), *M*(2), *M*(3) and *M*(6) octahedra share edges to form the F-wall (Fig. 5*a*), whereas in Sb-rich pinakiolite the F-wall is comprised of *M*(3) and *M*(6) edge-sharing octahedra (Fig. 5*b*). The largest difference between the F-walls of the two structures involves ordering of Sb^{5+}: in

TABLE 6. Site-scattering values (epfu) and assigned site-populations (apfu).

Site	Mult.[a]	SFAC[b]	SREF[c]	Sb^{5+}	Mn^{3+}	Al	Fe^{3+}	Mg	Mn^{2+}	□	epfu[d]
M(1)	1	Sb,Mg	41.6(3)	0.75				0.25			41.3
M(2)	1	Mg	8.9(4)					0.74		0.26	8.9
M(3)	1	Sb,Mg	23.6(3)	0.16				0.40	0.44		24.0
M(4)	1	Mn	22.8(3)		0.67	0.05		0.08	0.20		23.4
M(5)	1	Mn	23.2(3)		0.67		0.05	0.08	0.20		24.0
M(6)	1	Sb,Mg	18.1(4)	0.11				0.76	0.13		18.0
M(7)	2	Mn,Mg	32.4(5)					1.36	0.64		32.3
M(8)	2	Mn,Mg	33.9(5)					1.24	0.76		33.9
X(1)	1	Mn	9.6(5)*								
X(2)	2	Mn	8.1(6)*								
X(3)	2	Mn	8.4(4)*								42.9
X(4)	1	Mn	10.4(5)*					0.55*	1.45*		
X(5)	2	Mn	6.3(6)*								
Total			247.3	1.02	1.34	0.05	0.05	5.46	3.82	0.26	248.7

[a]Site multiplicity
[b]Assigned scattering factors
[c]Refined site-scattering values (epfu)
[d]Assigned electrons per formula unit [$Z = 1$]
*Total refined site-scattering over all *X* sites = 42.8 epfu attributed to ($Mn^{2+}_{1.45}Mg_{0.55}$)

TABLE 7. Bond-valence (in valence units) table for folvikite.

	O(1)	O(2)	O(3)	O(4)	O(5)	O(6)	O(7)	O(8)	O(9)	O(10)	Σ
M(1)						0.59 x2	0.85 x2	0.72 x2			4.32
M(2)			0.37 x2			0.24 x2	0.36 x2				1.94
M(3)			0.42 x2				0.38 x2	0.47 x2			2.54
M(4)	0.25 x2								0.75 x2	0.43 x2	2.86
M(5)		0.24 x2							0.73 x2	0.46 x2	2.86
M(6)			0.39 x2			0.31 x2		0.48 x2			2.36
M(7)	0.32	0.33		0.32	0.31			0.42	0.33		2.03
M(8)	0.33	0.31		0.31	0.33		0.46			0.32	2.06
B(1)	0.98	0.97	0.94								2.89
B(2)				1.00	0.97	0.83					2.80
X(1)					**0.30 x2**				**0.22 x2**	**0.45 x2**	1.94
X(2)					0.15				0.41	0.17	2.01
					0.44					0.84	
X(3)				0.43	0.40				0.50	0.96	2.29
X(4)				**0.29 x2**					**0.22 x2**	**0.44 x2**	1.90
X(5)				0.15					0.43	0.15	2.01
				0.39						0.89	
Σ	1.88	1.85	2.12	**1.92**	**1.91**	1.97	2.05	2.09	**2.25**	**2.10**	

*Using the bond-valence parameters of Brown and Altermatt (1985); all bond-valence multipliers (i.e. x2) apply to the summations at the cations; bond valences in bold font are for a simple *X*(1), *X*(4) ordered arrangement.

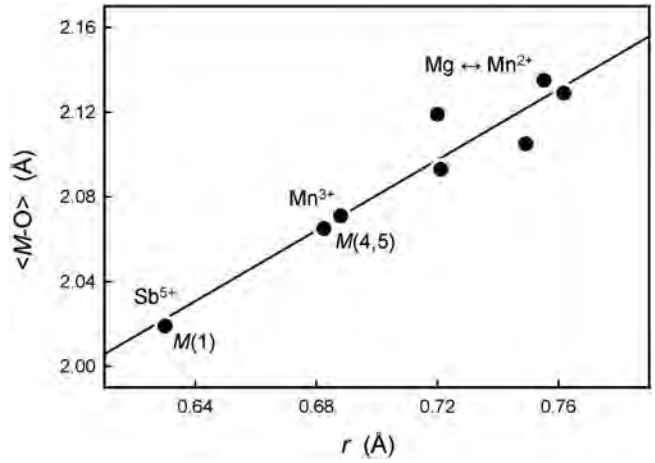

FIG. 4. The constituent radii for the *M*-site assignments *versus* the observed < *M*–O > distances for folvikite.

Sb-rich pinakiolite, the *M*(3) site is occupied by $Sb^{5+}_{0.38}Mn^{2+}_{0.32}Mg_{0.30}$, whereas in folvikite, the comparable octahedron strip has Sb^{5+} segregated differently between *M*(1) = ($Sb^{5+}_{0.75}Mg_{0.25}$) and *M*(3) = ($Mn^{2+}_{0.44}Mg_{0.40}Sb^{5+}_{0.16}$) (Table 6). This cation ordering at *M*(1) and *M*(3) in folvikite leads to a mean difference in octahedron size that is large enough to be visually discernible (Fig. 5*a*). Many zigzag-borate minerals bearing significant Sb (i.e. folvikite, Sb-rich pinakiolite and blatterite) have so far shown that all Sb is present as Sb^{5+} that occupies octahedrally coordinated sites within the F-wall (Norrestam and Hansen, 1990; Cooper and Hawthorne, 1998). We note here that the Sb_2O_5 content is essentially the

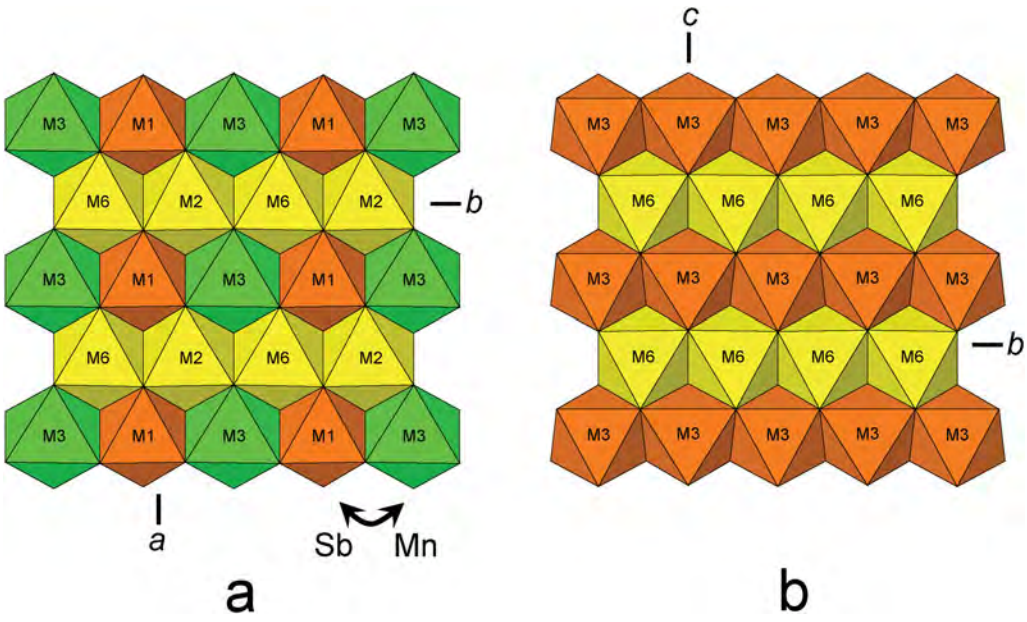

FIG. 5. The F-wall in: (*a*) folvikite and (*b*) Sb-rich pinakiolite. Yellow = (Mg > Mn^{2+}); green = (Mn^{2+} > Mg); and orange = Sb^{5+} dominant.

same for both folvikite (18.15 wt.%; Table 1) and Sb-rich pinakiolite (18.09 wt.%; Hansen *et al.*, 1988).

C-walls

The C-walls for folvikite and Sb-rich pinakiolite are shown in Figs. 6*a* and 6*b*, with simplified idealized (Mn^{2+},Mg) octahedra [*X*(1), *X*(4) in folvikite; *M*(4), *M*(5) in Sb-rich pinakiolite] occupying the disordered region between the Mn^{3+}-dominant strips of octahedra [*M*(4), *M*(5) in folvikite; *M*(1), *M*(2) in Sb-rich pinakiolite]. Although there are differences between the individual sites of the two structures (e.g. details of Jahn-Teller polyhedron distortions, Mn^{3+} content, Mn^{2+}/Mg ratio, occupancy of positionally disordered sites), the basic chemical prevalence at analogous sites is similar: the Jahn-Teller-distorted octahedra [*M*(4), *M*(5) in folvikite; *M*(1), *M*(2) in Sb-rich pinakiolite] are dominated by Mn^{3+}, and the intervening disordered cations [*X*(1) to *X*(5) in folvikite; *M*(4), *M*(5), *M*(45) in Sb-rich pinakiolite] are dominantly (Mn^{2+} > Mg), although folvikite is significantly enriched in Mn^{2+} relative to Sb-rich pinakiolite.

S-columns

The S-columns in both folvikite [*M*(7) and *M*(8)] and Sb-rich pinakiolite [*M*(7)] are dominated by Mg octahedra; however, folvikite contains ~⅔ Mg + ~⅓ Mn^{2+} at these octahedra, compared to octahedra fully occupied by Mg in Sb-rich pinakiolite.

Connectivity

The connectivity between F-walls, C-walls, S-columns and BO_3 groups is shown in Fig. 7 for folvikite (Fig. 7*a*) and Sb-rich pinakiolite (Fig. 7*b*). The general topology is the same for both minerals. The unit-cell translation 'up-the-page' for folvikite is ½ that of Sb-rich pinakiolite. In Sb-rich pinakiolite, successive C-walls along [100] are displaced by ½**y** relative to each other, such that Mn^{3+} octahedral strips alternate with disordered Mn^{2+}–Mg strips in a given (010) section (Fig. 7*b*). In folvikite, successive C-walls along [001] are not offset from each other in the (010) plane. Note that the $^{M(1)}Sb^{5+}$–$^{M(3)}Mn^{2+}$ ordering within the F-wall of folvikite is not apparent in Fig. 7*a* because only $^{M(1)}Sb^{5+}$ octahedra are present at the (010) level shown (cf. Fig. 5*a*).

The chemical formula of pinakiolite, Sb-rich pinakiolite and folvikite

Pinakiolite

The IMA Master List [http://nrmima.nrm.se//imalist.htm], gives the formula for pinakiolite as $(Mg,Mn)_2(Mn^{3+},Sb^{5+})O_2BO_3$, which is conveniently collapsed to a compact $O_2(BO_3)$ anion component ($Z = 8$). However, this formula lacks utility for Sb-bearing pinakiolites, as the Sb^{5+} content must be zero in order to maintain charge balance. The pinakiolite structure contains seven cation sites (other than B), of which three *Mn*(1–3) are clearly occupied by dominant Mn^{3+} and four *Mg*(1–4) by dominant Mg, providing $Mn^{3+}Mg_2$ pfu (Moore and Araki, 1974). The empirical formula for pinakiolite given by Moore and Araki (1974) is:

$$(Mg_{1.74}Mn^{3+}_{1.00}Mn^{2+}_{0.09}Mn^{4+}_{0.06}Al_{0.05}Fe^{3+}_{0.02}\square_{0.04})_{\Sigma 3}O_2(BO_3)$$

The pinakiolite formula can be written as $Mn^{3+}(Mg,Mn^{2+})_2O_2(BO_3)$ ($Z = 8$) for Sb-free pinakiolite.

Sb-rich pinakiolite

In Sb-rich pinakiolite, the *M*(3) site occupancy is reported as $(Sb_{0.38}Mn_{0.32}Mg_{0.30})$ with Sb dominant at the site. However, it was stated that the Mn and Mg contents at *M*(3) were not determined reliably (Norrestam and Hansen, 1990). The *M*(3) site has a <*M*(3)–O> distance of 2.05 Å, and applying our general relation between bond length and constituent radii <*M*–O> = 0.834(*r*) + 1.497 from folvikite, gives a constituent radius of 0.66 Å for the *M*(3) site in Sb-rich pinakiolite, which can be regarded as a good approximation for this homologous structure. Thus, the relatively short <*M*(3)–O> distance of 2.05 Å is not compatible with significant occupancy by the larger Mn^{2+} cation (0.83 Å radius, Shannon, 1976), and any Mn content must be dominated by Mn^{3+} (0.645 Å radius), as in pinakiolite. The individual *M*(3)–O bond lengths show very little variation in Sb-rich pinakiolite, and as Mn^{3+} is expected to induce bond-length distortions associated with Jahn-Teller effects, the absence of such a distortion indicates little or no Mn^{3+} at the *M*(3) site. The site occupancy reported for *M*(3) by Norrestam and Hansen (1990) is $(Sb_{0.38}Mn_{0.32}Mg_{0.30})$ which corresponds to a site-scattering of 30.98 electrons per site. If we exclude Mn from the *M*(3) site, this site-scattering value is concordant with the site occupancy $(Mg_{0.51}Sb_{0.49})$ which has an aggregate

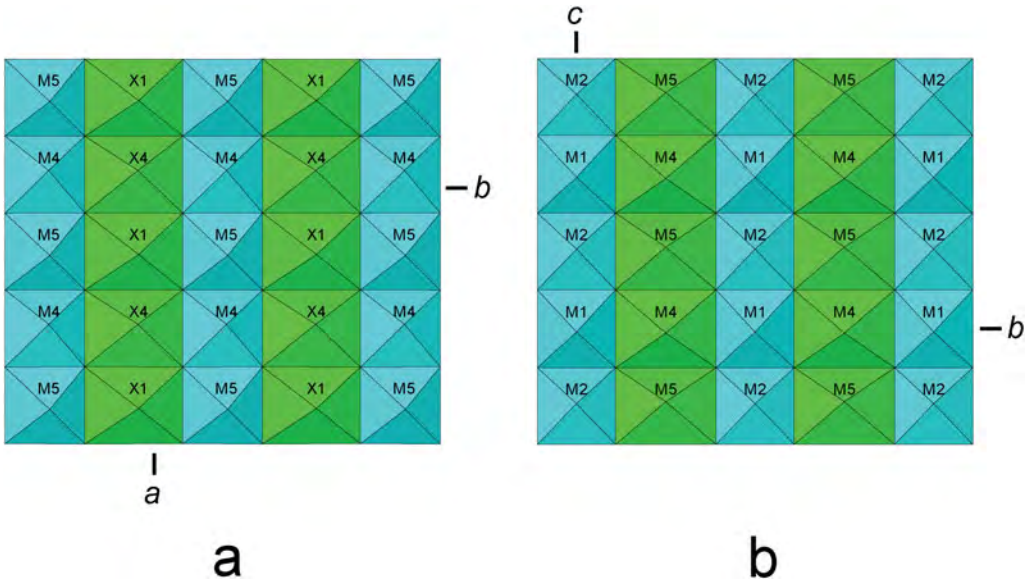

FIG. 6. The C-walls in: (*a*) folvikite and (*b*) Sb-rich pinakiolite. Blue = Mn^{3+} dominant and green = (Mn^{2+} > Mg).

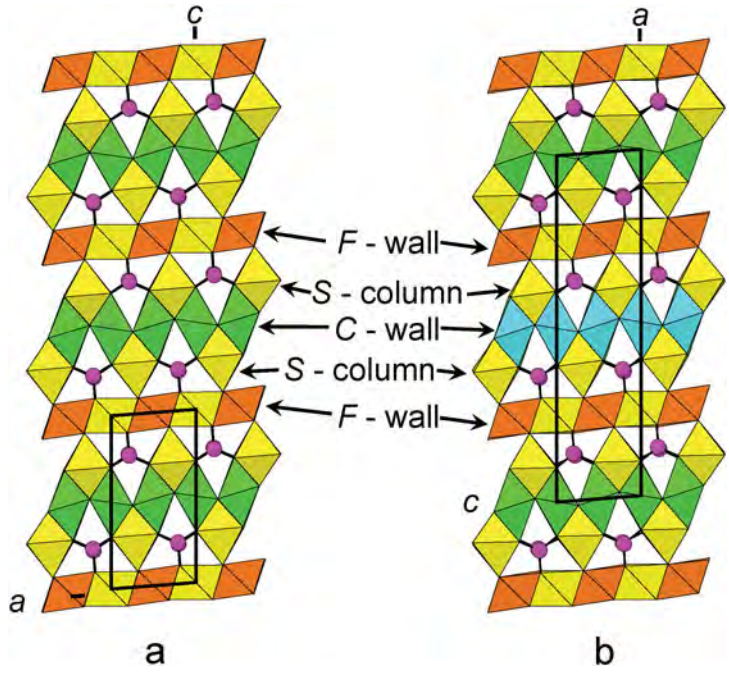

FIG. 7. The crystal structure of: (*a*) folvikite projected down [010]; (*b*) Sb-rich pinakiolite projected down [0$\bar{1}$0]. Legend as in Figs 5, 6; pink circles = B atoms.

TABLE 8. The differences between the *M* sites in Sb-rich pinakiolite and pinakiolite.

M sites	*M*(3)	*M*(1,2)	*M*(6,7)	*M*(4,45,5)	Anions	*Z*
Sb-rich pinakiolite	Mg,Sb^{5+}	Mn^{3+}	Mg_3	Mn^{2+},Mg	$O_4(BO_3)_2$	4
Pinakiolite	Mn_2^{3+}			Mg_4	$O_4(BO_3)_2$	4

ionic radius of 0.66 Å. We therefore suggest that only Sb^{5+} and Mg are present at *M*(3), and that all Mn^{3+} fully occupies the *M*(1) and *M*(2) sites, resulting in $Mn^{3+}_{0.5}$ pfu (*Z* = 8). The Sb-rich pinakiolite formula calculated using the electron-microprobe results of Hansen *et al.* (1988) with B = 1, Mn^{3+} = 0.5 and 5 anions pfu (*Z* = 8) gives:

$$(Mg_{1.691}Mn^{3+}_{0.5}Mn^{2+}_{0.448}Sb^{5+}_{0.238}Al_{0.009}Fe^{3+}_{0.002}\square_{0.112})_{\Sigma 3}O_2(BO_3)$$

The $Sb^{5+}_{0.238}$ content (pfu; *Z* = 8), if entirely ordered at the *M*(3) site, would result in an Sb^{5+} site-occupancy of 0.476, which is in good agreement with the $(Mg_{0.51}\ Sb_{0.49})$ site occupancy proposed above. Sb-rich pinakiolite is derived from pinakiolite via Sb^{5+} + Mg replacing Mn^{3+} at the *M*(3) site, with additional homovalent $Mn^{2+} \rightarrow$ Mg substitution occurring at the disordered *M* sites within the C-wall. An *M*(3) site fully occupied by Mn^{3+} (i.e. pinakiolite) would require substitution by ⅓ Sb^{5+} + ⅔ Mg to maintain charge balance, but the proposed *M*(3) site content of ~ $Sb_{0.5}$ exceeds this value, and an additional heterovalent substitution at another site(s) is required to achieve charge balance; this might involve divalent cations (Mn^{2+}, Mg) at the trivalent (Mn) *M*(1) and *M*(2) sites, and/

TABLE 9. Comparison of selected properties for folvikite and Sb-rich pinakiolite.

	Folvikite	Sb-rich pinakiolite
Locality	Nordmark, Sweden	Långban, Sweden
Habit	striated prisms	tabular platy crystals
Colour	black to reddish brown	light olive-green to yellow-brown
Lustre	submetallic	semimetallic
Space group	*P*2	*C*2/*m*
a (Å)	5.3767(10)	21.773(4)
b	6.2108(10)	6.153(2)
c	10.9389(18)	5.327(2)
β (°)	94.399(9)	94.38(2)
V (Å^3)	364.22(16)	711.6(4)
Z	1	4
$Density_{calc}$ (g cm^{-3})	4.14	3.92
Sb_2O_5	18.15	18.09
Mn_2O_3	11.62	18.54*
Fe_2O_3	0.45	0.06
Al_2O_3	0.27	0.22
MnO	29.73	14.93*
MgO	24.11	32.02
B_2O_3**	15.27	16.36
Total	99.60	100.22
Formula	$Sb^{5+}Mn^{3+}(Mg,Mn^{2+})_{10}O_8(BO_3)_4$	$(Mg,Sb^{5+})Mn^{3+}Mg_3(Mn^{2+},Mg)O_4(BO_3)_2$
References	This work	Hansen *et al*. (1988) Norrestam and Hansen (1990)

* Mn^{3+} / (Mn^{2+} + Mn^{3+}) adjusted to provide Mn^{3+} = 1 apfu; ** calculated using B = 4 (folvikite) and B = 2 apfu (Sb-rich pinakiolite).

or vacancies at the disordered *M*(4,45,5) sites within the C-wall. If we constrain the Sb^{5+} to occur at *M*(3) in subordinate fashion following the exchange ⅓ Sb^{5+} + ⅔ Mg → Mn^{3+}, we can convey the difference between pinakiolite and Sb-rich pinakiolite in the formula unit by reducing the *Z* value to 4, as shown in Table 8. The F-wall contains the *M*(3) and *M*(6) sites, the C-wall contains the ordered *M*(1) and *M*(2) sites and the disordered *M* (4–5) sites, and the S-column contains the *M*(7) site.

Folvikite

The *P*2 structure of folvikite contains a distinct Sb-dominant site, and the empirical formula $(Sb^{5+}_{1.02}Mn^{3+}_{1.34}Mg_{5.46}Mn^{2+}_{3.82}Al_{0.05}Fe^{3+}_{0.05}\square_{0.26})_{\Sigma 12}O_8(BO_3)_4$ can be simplified to $Sb^{5+}Mn^{3+}(Mg,Mn^{2+})_{10}O_8(BO_3)_4$ ($Z = 1$) to show the Sb^{5+} site-dominant character. In comparing folvikite with Sb-rich pinakiolite: (1) both have similar Sb_2O_5 content; (2) folvikite contains less Mn_2O_3 and MgO, but more MnO, relative to Sb-rich pinakiolite.

As is apparent from the above discussion, folvikite and Sb-rich pinakiolite are structurally and chemically quite similar; Table 9 compares selected properties of these two minerals. However, their habit and colour are quite distinct. Folvikite occurs as striated prisms whereas Sb-rich pinakiolite occurs as tabular platy crystals. Moreover, folvikite is black to reddish brown whereas Sb-rich pinakiolite is light olive-green to yellow-brown; presumably the additional Mg in Sb-rich pinakiolite serves to inhibit charge-transfer effects between heterovalent transition-metals.

Acknowledgements

Muriel Erambert assisted with the electron microprobe analysis, and the SEM BSE image was captured by Harald Folvik. We thank an anonymous referee, Tony Kampf, Pete Leverett and Principal Editors Peter Williams and Stuart Mills for their helpful comments on this paper. This work was supported by a Discovery grant from the Natural Sciences and Engineering Research Council of Canada and by grants from the Canada Foundation for Innovation to FCH.

Supplementary material

To view supplementary material for this article, please visit https://doi.org/10.1180/minmag.2017.081.059

References

Bartelmehs, K.L., Bloss, F.D., Downs, R.T. and Birch, J. B. (1992) Excalibr II. *Zeitschrift für Kristallographie*, **199**, 186–196.

Brown, I.D. and Altermatt, D. (1985) Bond-valence parameters obtained from a systematic analysis of the inorganic crystal structure database. *Acta Crystallographica*, **B41**, 244–247.

Burns, P.C., Cooper, M.A. and Hawthorne, F.C. (1994) Jahn-Teller distorted $Mn^{3+}O_6$ octahedra in fredriksso-nite, the fourth polymorph of $Mg_2Mn^{3+}(BO_3)O_2$. *The Canadian Mineralogist*, **32**, 397–403.

Cooper, M.A. and Hawthorne, F.C. (1998) The crystal structure of blatterite, $Sb^{5+}_3(Mn^{3+},Fe^{3+})_9(Mn^{2+},Mg)_{35}(BO_3)_{16}O_{32}$, and structural hierarchy in Mn^{3+}-bearing zigzag borates. *The Canadian Mineralogist*, **36**, 1171–1193.

Hansen, S., Hålenius, U. and Lindqvist, B. (1988) Antimony-rich pinakiolite from Långban, Sweden: a new structural variety. *Neues Jahrbuch für Mineralogie Monatshefte*, 231–239.

Hawthorne, F.C. and Grice, J.D. (1990) Crystal structure analysis as a chemical analytical method: application to light elements. *The Canadian Mineralogist*, **28**, 693–702.

Hawthorne, F.C., Ungaretti, L. and Oberti, R. (1995) Site populations in minerals: terminology and presentation of results of crystal-structure refinement. *The Canadian Mineralogist*, **33**, 907–911.

Holland, T.J.B. and Redfern, S.A.T. (1995) Unit cell refinement from powder diffraction data: the use of regression diagnostics. *Mineralogical Magazine*, **61**, 65–77.

Magnusson, N.H. (1929) Nordmarks malmtrakt. Geologisk beskrivning. *Sveriges Geologiska Undersökning, Serie Ca*, **13**, 98 pp.

Mills, S.J., Christy, A.G., Chen, E.C.C. and Raudsepp, M. (2009) Revised values of the bond valence parameters for [6] Sb (V)–O and [3–11] Sb (III)–O. *Zeitschrift für Kristallographie*, **224**, 423–431.

Moore, P.B. and Araki, T. (1974) Pinakiolite, $Mg_2Mn^{3+}O_2[BO_3]$; warwickite, $Mg(Mg_{0.5}Ti_{0.5})O[BO_3]$; wightma-nite, $Mg_5(O)(OH)_5[BO_3]\cdot nH_2O$: crystal chemistry of complex 3 Å wallpaper structures. *American Mineral-ogist*, **59**, 985–1004.

Norrestam, R. and Hansen, S. (1990) Structural investigation of an antimony-rich pinakiolite, $Mg_{1.90}Mn_{0.91}Sb_{0.19}O_2BO_3$, from Långban, Sweden. *Zeits-chrift für Kristallographie*, **191**, 105–116.

Raade, G. and Folvik, H. (2013) On an unnamed Mg–Mn–Sb oxyborate from the blatterite locality of the Kitteln mine, Nordmark, Filipstad, Värmland, Sweden. *Norsk Bergverksmuseum Skrift*, **50**, 49–54.

Raade, G., Mladeck, M.H., Din, V.K., Criddle, A.J. and Stanley, C.J. (1988) Blatterite, a new Sb-bearing Mn^{2+} – Mn^{3+} member of the pinakiolite group, from Nordmark,

Sweden. *Neues Jahrbuch für Mineralogie Monatshefte*, 121–136.

Rowe, R. (2009) New statistical calibration approach for Bruker AXS D8 Discover microdiffractometer with Hi-Star detector using GADDS software. *Powder Diffraction*, **24**, 263–271.

Shannon, R.D. (1976) Revised effective ionic radii and systematic studies of interatomic distances in halides and chalcogenides. *Acta Crystallographica*, **A32**, 751–767.

Sjögren, A. (1876) Mineralogiska notiser. III. Manganosit och pyrochroit funna i Mossgrufvan Å Nordmarksfältet i Vermland. *Geologiska Föreningens i Stockholm Förhandlingar*, **3**, 181–183.

Sjögren, A. (1878) Mineralogiska notiser. V. Manganförekomsten i Nordmarken. *Geologiska Föreningens i Stockholm Förhandlingar*, **4**, 156–163.

Sjögren, A. (1887) Mineralogiska notiser. XIII. Om Nordmarks-periklasen. *Geologiska Föreningens i Stockholm Förhandlingar*, **9**, 526–532.

Strunz, H. and Nickel, E.H. (2001) *Strunz Mineralogical Tables. 9th Edition*. E. Schweizerbart'sche Verlagsbuchhandlung, Stuttgart. 870 pp.